Supplementary information

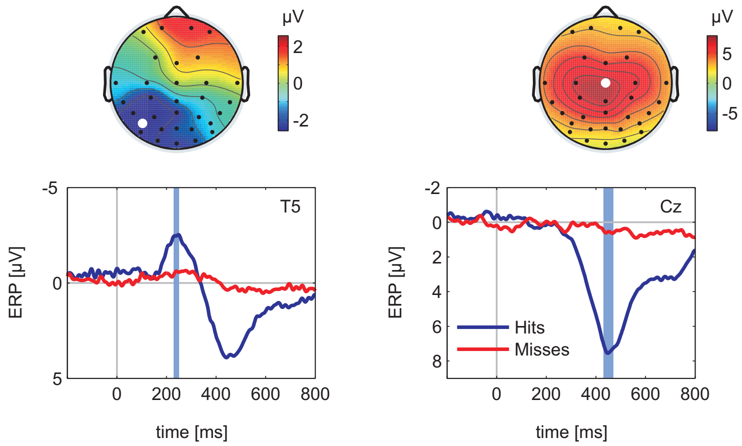

Supplementary Figure 1: Event–related potentials (ERPs; grand average over 12 subjects). Left: ERP time course at electrode T5 and topography in the time range shaded in blue (230 – 250 ms). Right: ERP time course at electrode Cz and topography in the time range 430 – 470 ms.

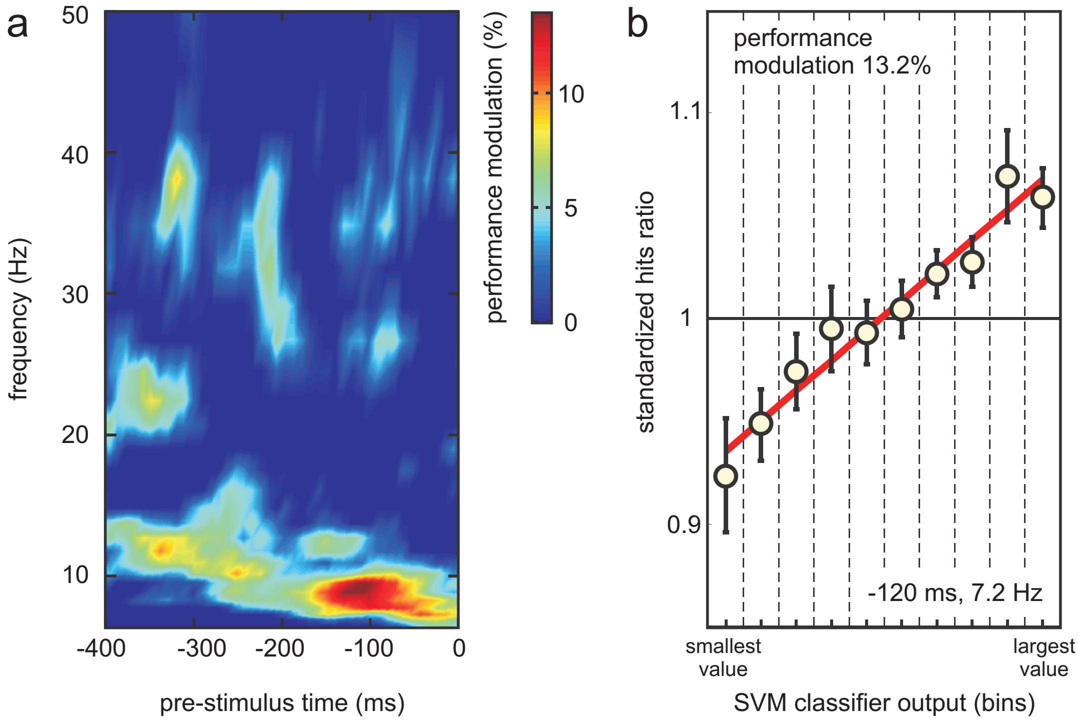

Supplementary Figure 2: For each subject, we repeated the following procedure 20 times. At each time-frequency point within the range of 4 – 50 Hz and -400 – 0 ms pre–stimulus, we trained a linear Support Vector Machine classifier to discriminate hits and misses based on the corresponding phase at electrode Fz (represented as a unit–length vector in the 2D complex plane). Label -1 was assigned to miss trials and label +1 to hit trials. Training was performed on a randomly selected subset of 80% of trials and repeated 5 times, each time leaving out another 20% of trials, resulting in a full cross–validation procedure. The classifier was then tested on the remaining 20% of trials of the dataset: for each trial, it would return a decision value (a number usually between -1 and 1) and would use the sign of that decision value to predict a label for the test trial. If phase information does allow the classifier to reliably generalize from the training set to the test set, then the subject's hit rate should be correlated with these decision values. We thus organized decision values into 10 bins, and for each bin, computed the standardized hit rate of the subject over the corresponding trials. We quantified the influence of phase information on detection performance as the slope of the best–fitting line linking the binned classifier output decision value to the standardized hit rate. This slope was averaged over the 5 repetitions of the 5–fold cross–validation and over the 20 repetitions of the entire procedure, and the result finally averaged over subjects. An example is shown in panel b for the time–frequency point giving the maximum phase effect in our study: 7 Hz and -120ms. The grand–average map of performance modulation by phase information at each time–frequency point is shown in panel a. This independent analysis thus confirms the main result of our study (Fig 3b in the main manuscript), i.e. that phase information around 7 Hz shortly before stimulus onset can affect the subsequent detection performance (here with a maximum modulation amplitude of about 14%).

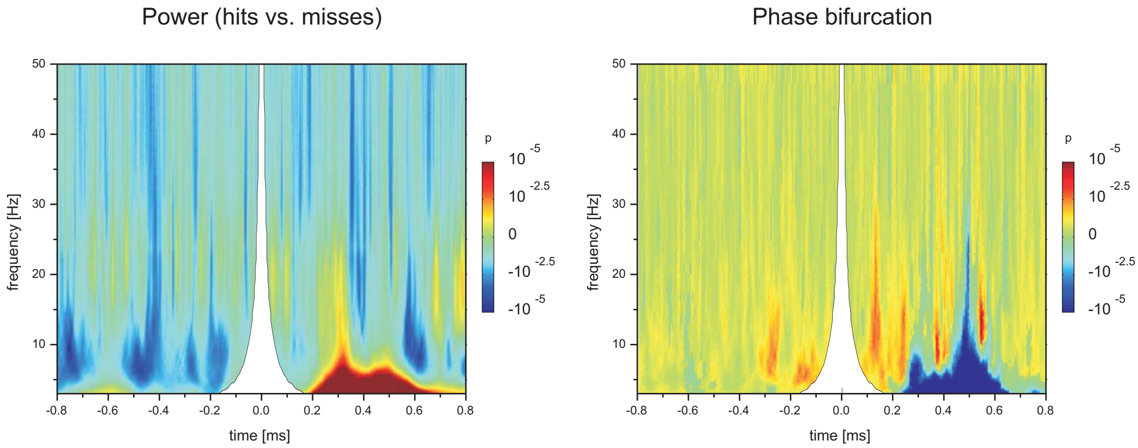

Supplementary Figure 3: Statistical significance of power differences (left) and phase bifurcation (right) between hits and misses at electrode Fz. Analyses similar to those displayed in Figure 2 were performed, but using a wavelet with a length of only one cycle for each frequency. The white filled area masks the time range in which prestimulus and poststimulus effects could have been potentially confounded due to the wavelet transform. The main results from the previous analysis using a longer wavelet are confirmed here, indicating that effects in the prestimulus time window were not due to contamination with poststimulus data.

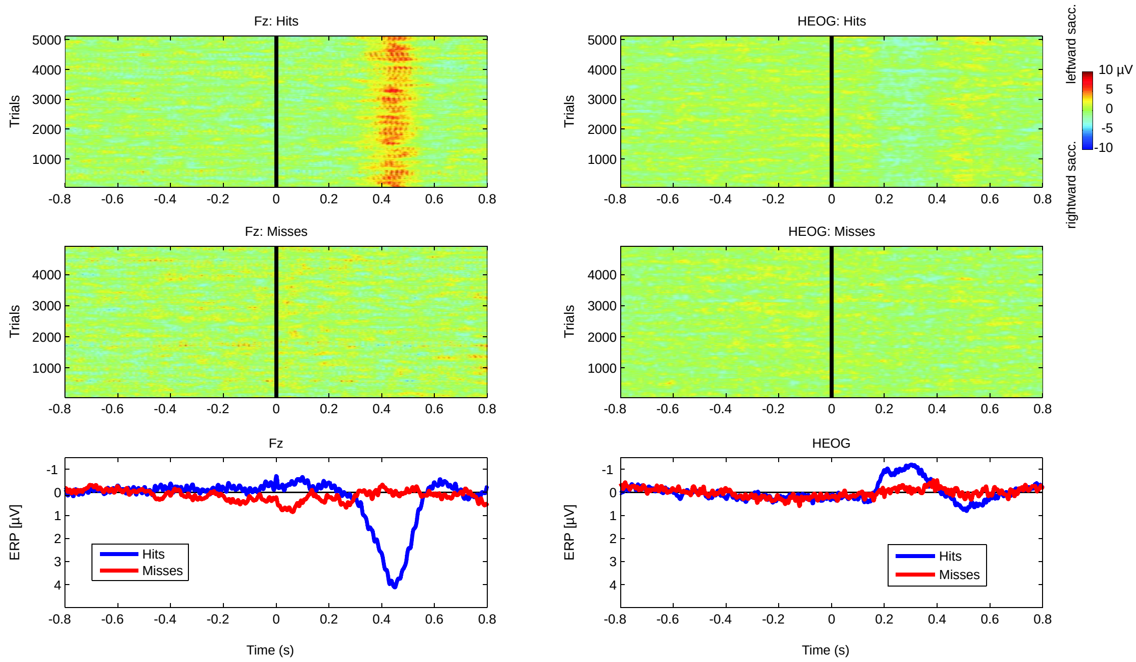

Supplementary Figure 4: Results at channel Fz (left) and the horizontal electrooculogram (HEOG; right). In the top four panels, each colored horizontal trace represents a single-trial (low–pass filtered at 100 Hz) whose potential variations are color–coded (data are plotted for all subjects). A moving average across 100 adjacent single trials was applied vertically to highlight trial–to–trial consistencies. The bottom two panels show the grand–averaged event–related potential (ERP). We investigated whether prestimulus effects were possibly affected by ocular artifacts. For example, differences in power and phase on hit and miss trials could have simply been caused by differences in the number or the timing of eye blinks prior to stimulus onset. Eye blinks are associated with high amplitude signals at frontal channels. However, we found no evidence for eye blinks on single trials or in the average ERP, either at Fz (where power and phase bifurcation effects were strongest) or in the HEOG (cf. supplementary Figure S3), for hits or misses. Alternatively, hits and misses might have been associated with horizontal saccades towards or away from the target, respectively. If so, these saccades might have introduced an electrical artifact with opposite polarity (i.e. opposite phase angles) for hits and misses. However, inspection of the HEOG on single trials and in the averaged ERP did not reveal any signs of systematic prestimulus saccades, least of all in opposite directions (cf. supplementary Figure S4). The HEOG is sensitive to macro–saccades down to a few degrees visual angle (Hillyard and Galambos, 1970; Lins et al., 1993). We cannot exclude, however, the possibility that the data might be contaminated by artifacts caused by a number of smaller saccades, i.e. so–called micro–saccades, defined as very short saccades of less than 1° (Martinez-Conde et al., 2004). However, such artifacts have generally been reported to affect mostly higher frequencies (i.e. above 20 Hz; Trujillo et al., 2005; Yuval-Greenberg et al., 2008). In sum, these results indicate that power and phase bifurcation effects in the main analysis were not brought about by ocular artifacts.

References

Hillyard SA, Galambos R (1970) Eye movement artifact in the CNV. *Electroencephalogr Clin Neurophysiol* 28:173–182.

Lins OG, Picton TW, Berg P, Scherg M (1993) Ocular artifacts in EEG and event-related potentials. I: Scalp topography. *Brain Topogr* 6:51–63.

Martinez-Conde S, Macknik SL, Hubel DH (2004) The role of fixational eye movements in visual perception. *Nat Rev Neurosci* 5:229–240.

Trujillo LT, Peterson MA, Kaszniak AW, Allen JJB (2005) EEG phase synchrony differences across visual perception conditions may depend on recording and analysis methods. *Clin Neurophysiol* 116:172–189.

Yuval-Greenberg S, Tomer O, Keren AS, Nelken I, Deouell LY (2008) Transient induced gamma-band response in EEG as a manifestation of miniature saccades. *Neuron* 58:429–441.